24th COBEM - 2017

24th ABCM International Congress of Mechanical Engineering
December 3-8, 2017, Curitiba, PR, Brazil

COBEM-2017-1545
A HYPERBOLIC - REGULARIZED CASSON MODEL FOR PULSATILE BLOOD FLOW SIMULATION IN A RIGID ARTERY

Fábio Allan Cruz Martelli
Pedro Oliveira Carvalho da Silva
Federal University of Pará, Mechanical Engineering School, Belém, Brazil
fabiomartelli7@gmail.com
pedro.0106@gmail.com

Emanuel Negrão Macêdo
Federal University of Pará, Chemical Engineering School, Belém, Brazil
enegrao@ufpa.br

Abstract. *The behavior of blood flow inside an artery is very difficult to describe due to the fact that it is constantly being pumped by the heart and is subjected to several factors, such as non-Newtonian viscosity, variation of the pressure and velocity gradients, body acceleration and so forth. All those factors make it a challenge to develop a mathematical model capable of describing all these physical phenomena. This work aims to develop a model in terms of a basic viscoelastic fluid flow under the effect of the Jeffreys model, and a regularized Casson model for viscosity. To solve this problem, the hyperbolic equation was implemented both in the symbolic manipulation software, Wolfram Mathematica, and in the FORTRAN software, where the effects of relaxation and retardation times and of the yield stress are used as basis for cases simulations. The model was successfully simulated and its parameters were satisfactorily observed, showing a good agreement with a previously known limit case.*

Keywords: *Blood flow, Jeffreys, Regularized Casson, Hyperbolic model.*

1. INTRODUCTION

The search for understanding the behavior patterns of the blood flow in the human body is of great interest in Medicine and Biomedical Engineering; it is an important branch in the research and diagnosis of some cardiovascular diseases. Blood is considered to be one of the most important biological multi-component mixtures occurring in nature. It is composed of plasma, red and white blood cells, platelets etc. Constitutive modeling of blood has received much attention due to the fact that the flow characteristics of blood influence many of the pathological conditions observed in the cardiovascular system (Fung, 1993; Humphrey and Delange, 2004; Massoudi and Phuoc, 2008).

In the past few years, the growth and advancement of Biomedical Engineering and Medical Science have become visible, especially when it comes to the creation or perfectioning of the methods that seek to ease certain medical procedures, such as the improvement of the efficiency of the treatment by intra-arterial medication. For such, there is a need to develop a model that is able to describe the behavior of blood flow inside its vessels. It must take into account several aspects such as the periodic pressure gradient, the viscosity of the fluid and even the action of external forces caused by body acceleration (Chaturani and Palanisamy,1990).

In the past few years, many studies on pulsatile flow of non-Newtonian fluids have been done. These include an important work proposed by Chaturani and Palanisamy (1990) that treats the pulsatile flow of a power-law fluid through rigid circular tubes under the influence of a periodic body acceleration. In this work, interaction of non-Newtonian nature of fluid with the body acceleration has been investigated by using the physiological data for two particular cases (coronary and femoral arteries). The axial velocity, fluid acceleration, wall shear stress and instantaneous volume flow rate have been computed and their variations with different parameters have been analyzed. Gahemi, *et al.* (2016) analyzed numerically the flow for a non-Newtonian third grade blood in coronary and femoral arteries. Blood is considered as a third grade non-Newtonian fluid under periodic body acceleration motion and pulsatile pressure gradient; Misra and Pal (1999) studied the laminar pulsatile flow of blood under the influence of externally imposed body accelerations. A mathematical model is developed by treating blood as a non-Newtonian fluid, using a biviscosity model for blood. The governing equations are solved by using finite-difference technique. Closed form solutions by Laplace transformations are also obtained for the low pulse frequency region and these solutions are compared with the other results. In Massoudi and Phuoc (2008), a study is presented on the unsteady pulsatile flow of blood in an artery, where the effects of body

acceleration are included. The blood is modeled as a modified second-grade fluid where the viscosity and the normal stress coefficients depend on the shear rate. It is assumed that the blood near the wall behaves as a Newtonian fluid, and in the center as a non-Newtonian fluid. This phenomenon is also known as the Fahraeus–Lindqvist effect. The equations are made dimensionless and solved numerically.

In this context, the objective of this work is to present a mathematical model for the blood flow in an artery, with pressure gradient varying periodically in time. In this mathematical formulation, the Jeffreys viscoelastic model (Bird, 2007) was used to evaluate the effect of the periodic pressure gradient, along with the Casson - Regularized model for fluid viscosity (Papanastasiou, 1987; Mitsoulis, 2007). To do so, the Wolfram Mathematica and FORTRAN softwares was used to solve the hyperbolic governing equation based on a Jeffreys - Regularized Casson model able to study the effects of periodic pressure gradient and fluid viscosity in the flow characteristics.

2. MATHEMATICAL FORMULATION

The physical problem consists of the transient, laminar, pulsatile, axisymmetric and fully developed blood flow through a rigid circular duct that can be subjected to a body force. The blood will be represented mathematically by two rheological models, Jeffreys viscoelastic model for the shear stress (Bird, 2007) and Casson regularized by Papanastasiou (Papanastasiou, 1987; Mitsoulis, 2007) for the blood apparent viscosity. From these considerations, we obtain the following equations and boundary conditions:

$$\begin{cases} \rho\left(\lambda_0 \dfrac{\partial^2 u}{\partial t^2} + \dfrac{\partial u}{\partial t}\right) = F + \dfrac{1}{r}\dfrac{\partial}{\partial r}\left(r\mu\dot{\gamma}\right) + \dfrac{\lambda_1}{r}\dfrac{\partial}{\partial r}\left(r\mu\dfrac{\partial \dot{\gamma}}{\partial t}\right) \\ t = 0 \Rightarrow u = \dfrac{\partial u}{\partial t} = 0 \\ r = 0 \Rightarrow \dfrac{\partial u}{\partial r} = 0;\ r = R_w \Rightarrow u = 0 \end{cases} \tag{1.a-e}$$

Being u is the velocity field of the flow, r is the radial variable, R_w is the radius of the duct, ρ is the specific mass, μ is the apparent Casson viscosity, t is the time, λ_0 is the Jeffreys relaxation time and λ_1 is the Jeffreys retardation time. In addition, some of the other symbols are defined as follows:

$$\dot{\gamma} = \frac{\partial u}{\partial r};\quad F = f + \lambda_0 \frac{\partial f}{\partial t};\quad f = \Delta P + \rho G$$

$$\Delta P = -\frac{\partial P}{\partial z} = A_0 + A_1 \cos\left(\omega_p t\right);\quad G = a_0 \cos\left(\omega_b t + \phi\right);\quad \omega_p = 2\pi f_p;\quad \omega_b = 2\pi f_b \tag{2.a-h}$$

$$\mu\left(\dot{\gamma}\right) = \begin{cases} \left[\sqrt{\mu_0} + \sqrt{\dfrac{\tau_0}{|\dot{\gamma}|}}\left(1 - e^{-\sqrt{m|\dot{\gamma}|}}\right)\right]^2, \text{ if } \dot{\gamma} \neq 0 \\ \left(\sqrt{\mu_0} + \sqrt{m|\dot{\gamma}|}\right)^2, \text{ if } \dot{\gamma} = 0 \end{cases}$$

In which ΔP is the pressure gradient, G is the body acceleration, ϕ is the lead angle, f_p is the pulse rate frequency, f_b is the body acceleration frequency, m is the regularization parameter (Papanastasiou, 1987; Mitsoulis, 2007) and τ_0 is the yield stress.

The average velocity is determined by:

$$u_{av} = \frac{2}{R_w^{\,2}} \int_0^{R_w} r \cdot u(t, r)\, dr \tag{3}$$

Another important property to determine is the Fanning friction factor (Bird, 2007), which is defined as:

$$F_f = \frac{\Delta P\, R_w}{\rho\, u_{av}^{\,2}} \tag{4}$$

It is also possible to quantify the improvement of the pulsatile flow in relation to the flow without pressure variation. According to Hernandez-Martinez (2012), the improvement in the flow rate and improvement in the friction factor can be calculated as follows:

$$IQ = \frac{u_{av\ \text{cossine pressure}} - u_{av\ \text{constant pressure}}}{u_{av\ \text{constant pressure}}}; \qquad IF_f = \frac{F_{f\ \text{cossine pressure}} - F_{f\ \text{constant pressure}}}{F_{f\ \text{constant pressure}}} \tag{5.a, b}$$

3. NONDIMENSIONALIZATION OF THE PROBLEM

The nondimensionalization of the equations that govern the blood flow, as well as the boundary and initial conditions, is done from the following dimensionless groups:

$$t^* = t\,f_p;\ \ \eta = \frac{r}{R_w};\ \ U = \frac{u}{u_r};\ \ \dot{\Gamma} = \frac{R_w\dot{\gamma}}{u_r};\ \ \tilde{\mu}\left(\dot{\Gamma}\right) = \frac{\mu\left(\dot{\gamma}\right)}{\mu_0};\ \ M = \frac{m u_r}{R_w};\ \ Y_0 = \frac{\tau_0 R_w}{\mu_0 u_r};\ \ \tilde{\rho} = \frac{\rho}{\rho_0};\ \ \tau_{R0} = \lambda_0 f_p$$
$$\tau_{R1} = \lambda_1 f_p;\ \ \mathrm{Re} = \frac{\rho_0 u_r D_H}{\mu_0};\ \tilde{F} = \frac{F}{\rho_0 u_r f_p}\ ;\ \tilde{f} = \frac{f}{\rho_0 u_r f_p};\ \ \Delta\tilde{P} = \frac{\Delta P}{\rho_0 u_r f_p};\ \ \tilde{G} = \frac{G}{u_r f_p} \tag{6.a-u}$$
$$\tilde{A}_0 = \frac{A_0}{\rho_0 u_r f_p};\ \tilde{A}_1 = \frac{A_1}{\rho_0 u_r f_p};\ \ e = \frac{\tilde{A}_1}{\tilde{A}_0};\ \ \omega_r = \frac{\omega_b}{\omega_p};\ \ \tilde{a}_0 = \frac{a_0}{u_r f_p};\ \alpha = \frac{\mu_0 u_r}{R_w{}^2 \rho_0 u_r f_p} = \frac{4u_r}{\mathrm{Re}\, f_p D_H}$$

The dimensionless equations (1-5) are presented as follows:

$$\begin{cases} \tilde{\rho}\left(\tau_{R0}\dfrac{\partial^2 U}{\partial t^{*2}} + \dfrac{\partial U}{\partial t^*}\right) = \tilde{F} + \dfrac{\alpha}{\eta}\dfrac{\partial}{\partial\eta}\left(\eta\tilde{\mu}\dot{\Gamma}\right) + \tau_{R1}\dfrac{\alpha}{\eta}\dfrac{\partial}{\partial\eta}\left(\eta\tilde{\mu}\dfrac{\partial\dot{\Gamma}}{\partial t^*}\right) \\ t^* = 0 \Rightarrow U = \dfrac{\partial U}{\partial t^*} = 0 \\ \eta = 0 \Rightarrow \dfrac{\partial U}{\partial\eta} = 0;\ \eta = 1 \Rightarrow U = 0 \end{cases} \tag{7.a-e}$$

$$\dot{\Gamma} = \frac{\partial U}{\partial\eta};\ \ \tilde{F} = \tilde{f} + \tau_{R0}\frac{\partial\tilde{f}}{\partial t^*};\ \ \tilde{f} = \Delta\tilde{P} + \tilde{\rho}\tilde{G};\ \ \Delta\tilde{P} = \tilde{A}_0\left[1 + e\cos\left(2\pi t^*\right)\right];\ \ \tilde{G} = \tilde{a}_0\cos\left(2\pi\omega_r t^* + \phi\right)$$
$$\tilde{\mu}\left(\dot{\Gamma}\right) = \begin{cases} \left[1 + \sqrt{\dfrac{Y_0}{\left|\dot{\Gamma}\right|}}\left(1 - e^{-\sqrt{M\left|\dot{\Gamma}\right|}}\right)\right]^2, \text{ if } \dot{\Gamma} \neq 0 \\ \left(1 + \sqrt{M\left|\dot{\Gamma}\right|}\right)^2, \text{ if } \dot{\Gamma} = 0 \end{cases} \tag{7.f-k}$$

The average velocity, Fanning friction factor, improvement in the flow rate and the improvement in fRe (Friction factor times Reynolds) are given by

$$U_{av}\left(t^*\right) = 2\int_0^1 \eta U\left(t^*,\eta\right) d\eta\,; \qquad \mathrm{Re}F_f = \frac{2}{\alpha}\frac{\Delta\tilde{P}}{\tilde{\rho}U_{av}{}^2} \tag{8.a, b}$$

$$IQ = \frac{U_{av\ \text{cossine pressure}} - U_{av\ \text{constant pressure}}}{U_{av\ \text{constant pressure}}}; \qquad I\mathrm{Re}F_f = \frac{\mathrm{Re}F_{f\ \text{cossine pressure}} - \mathrm{Re}F_{f\ \text{constant pressure}}}{\mathrm{Re}F_{f\ \text{constant pressure}}} \tag{8.c, d}$$

4. SOLUTION METHODOLOGY

4.1 Mathematica

For the solution of the proposed problem, the dimensionless equations presented were implemented in the Mathematica symbolic manipulation software. The NDSolve routine was used to find the solution of the differential equation. NDSolve returns as a result an interpolation function, and solves a wide range of ordinary differential equations and many partial differential equations (Wolfram, 2017). The Method of Lines was chosen as the solution method in the NDSolve routine. This method is a numerical procedure that consists in approaching spatial dependencies by finite difference formulas, leaving the differential equation and its boundary conditions as a function of time. Once this is done,

the software integrates the initial value ODE system to solve the problem. The type of spatial discretization chosen was that of the Tensor Product Grid, present in the software itself.

4.2 Fortran

For the implementation of the system in FORTRAN, a discretization was made in the spatial variable by the finite volume method. This method uses mass balance, energy and momentum in a continuous medium volume to solve the differential equations of a system (Maliska, 2004).

The formulation was done as follows:

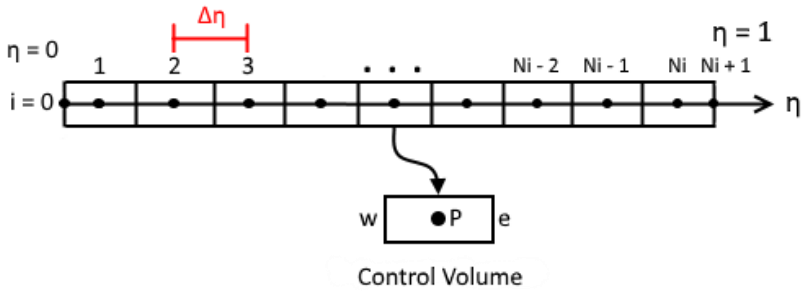

Figure 1. Schematic of the discretization of the system.

It was defined that the distance between the centers of each control volume is given by $\Delta\eta = {}^{1}\!/_{Ni}$, being Ni is the number of intervals chosen. For a large number of intervals, we can assume that, in a given control volume, $\tilde{\rho} \approx \tilde{\rho}_P$, $U \approx U_P$ e $\tilde{F} \approx \tilde{F}_P$. Applying the PDE in the control volume and integrating it from "w" to "e" (Fig. 1) as a function of η, we obtain the following expression for any volume between 1 and Ni:

$$\begin{cases} B\tilde{\rho}_P\tau_{R0}\dfrac{d^2U_P}{dt^{*2}} + \left[B\tilde{\rho}_P + \alpha\tau_{R1}\left(\beta_e+\beta_w\right)\right]\dfrac{dU_P}{dt^*} = B\tilde{F}_P + \alpha\left[\beta_w U_W - \left(\beta_e+\beta_w\right)U_P + \beta_e U_E\right] + \alpha\tau_{R1}\left[\beta_w\dfrac{dU_W}{dt^*} + \beta_e\dfrac{dU_E}{dt^*}\right] \\ t^* = 0 \Rightarrow U_P = 0;\ \dfrac{dU_P}{dt^*} = 0 \\ B = \dfrac{1}{2}\left(\eta_e^{\,2} - \eta_w^{\,2}\right);\quad \beta_{e,w} = \dfrac{\left(\eta\tilde{\mu}\right)_{e,w}}{\Delta\eta} \end{cases} \tag{9.a-e}$$

For the first volume (i = 1), there is a specification in the equation:

$$\begin{cases} \eta_e = \Delta\eta;\quad \eta_w = 0 \\ B\tilde{\rho}_P\tau_{R0}\dfrac{d^2U_P}{dt^{*2}} + \left[B\tilde{\rho}_P + \alpha\tau_{R1}\beta_e\right]\dfrac{dU_P}{dt^*} = B\tilde{F}_P + \alpha\beta_e\left(U_E - U_P\right) + \alpha\tau_{R1}\beta_e\dfrac{dU_E}{dt^*} \end{cases} \tag{9.f-h}$$

The same occurs for the last volume (i = Ni):

$$\begin{cases} \eta_e = 1;\quad \eta_w = 1 - \Delta\eta \\ B\tilde{\rho}_P\tau_{R0}\dfrac{d^2U_P}{dt^{*2}} + \left[B\tilde{\rho}_P + \alpha\tau_{R1}\left(\beta_e+\beta_w\right)\right]\dfrac{dU_P}{dt^*} = B\tilde{F}_P + \alpha\left[\beta_w U_W - \left(\beta_e+\beta_w\right)U_P\right] + \alpha\tau_{R1}\beta_w\dfrac{dU_W}{dt^*} \end{cases} \tag{9.i-k}$$

Afterwards, they were implemented in the FORTRAN software and solved using the International Mathematical and Statistical Library (IMSL, 2014) routines, more specifically the IVPAG routine. The CSINT (for data interpolation) and CSITG (for integration) routines were used to perform the integrations of Uav, IQav and $IReFf_{av}$.

5. RESULTS

The conditions applied in the system and the simulated cases are the same in Mathematica and FORTRAN. However, some cases were also simulated for a more complete analysis of the effect of the Y_0 (dimensionless yield stress), τ_{R0}

(dimensionless relaxation time) and τ_{R1} (dimensionless retardation time). A mesh convergence analysis was performed, in the Mathematica and FORTRAN codes, and it was observed that 200 intervals obtained convergence in three significant digits.

Different cases were computed for different flow situations in order to obtain a basis for the analysis of the results. In all cases, it was considered that there is no body force acting on the flow (G = 0), the relationship between A_1 and A_0 is 0.2 (e = A1/A0 = 0.2), the regularization parameter for the Casson's model "M" was assumed equal to 1, the dimensionless specific mass adopted was 1 ($\rho = 1$) and the dimensionless parameter $\alpha = 1/8$. In addition, the dimensionless simulation time was 3π.

To carry out the verification of the proposed model, we will compare the results obtained here with those obtained by the analytical solution of the limit case when $Y_0 = 0$, $\tau_{R0} = 0$, $\tau_{R1} = 0$ and A1 = 0 (or e = 0). The analytical solution for this limit case is given by:

$$\begin{cases} U(t^*,\eta) = \dfrac{A_0}{4\alpha}(1-\eta^2) - \dfrac{A_0}{\alpha}\displaystyle\sum_{i=1}^{N} \frac{J_2(\mu_i)}{\mu_i^2 J_1^2(\mu_i)} J_0(\mu_i \eta)\, \mathrm{e}^{-\alpha\mu_i^2 t^*}; \quad U_{av}(t^*) = \frac{A_0}{\alpha}\left(\frac{1}{8} - 2\sum_{i=1}^{N} \frac{J_2(\mu_i)}{\mu_i^3 J_1(\mu_i)} \mathrm{e}^{-\alpha\mu_i^2 t^*}\right) \\ \mathrm{Re}\, F_f = \dfrac{128\alpha}{A_0} \dfrac{1}{\left(1 - 16\displaystyle\sum_{i=1}^{N} \frac{J_2(\mu_i)}{\mu_i^3 J_1(\mu_i)} \mathrm{e}^{-\alpha\mu_i^2 t^*}\right)^2}; \quad \text{being } \mu_i \text{ the root of } J_0(\mu_i) = 0 \end{cases} \tag{10.a-d}$$

It can be seen from equation (10.c) that for $t^* \to \infty$, $A_0 = 1$ and $\alpha = 1/8$, the product Reynolds times friction factor (ReF_f) tends to 16 (i.e., $f_f = 16 / Re$). Such a result is bound for flow in a circular duct.

To validate the results obtained by the codes developed here (Mathematica and FORTRAN), Figs. 2 and 3 are presented. In Fig. 2 the results of (a) $U(t^*, \eta)$ versus t^* with varying η and (b) $U(t^*, \eta)$ versus η with varying t^* are shown. It is observed a perfect agreement between the results obtained by the two codes. In Fig. 2.a it is noted that the oscillations in velocity, due to the periodic pressure gradient, are attenuated by the action of the viscous effects as it approaches the duct wall.

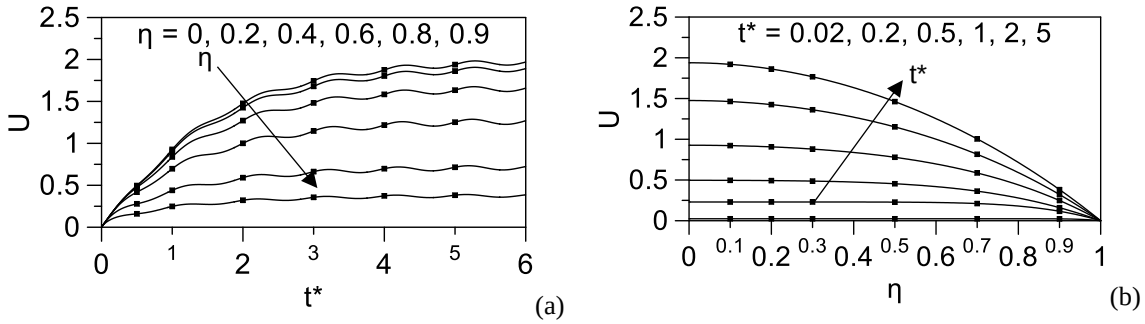

Figure 2. a, b - Comparison between the results obtained by Mathematica (dots) and FORTRAN (lines) for the reference case
($Y_0 = 0$, $\tau_{R0} = 0$, $\tau_{R1} = 0$). The arrow indicates the direction of increase of the third variable.

In Figs. 3.a, b is presented the comparison of the results obtained with Mathematica and FORTRAN codes, for the improvement in the flow rate (IQ) and the improvement in fRe (IF) in function of the time variable. Therefore, Figs. 2 and 3 show that both softwares were capable of computing the physical problem and are in agreement regarding the results obtained.

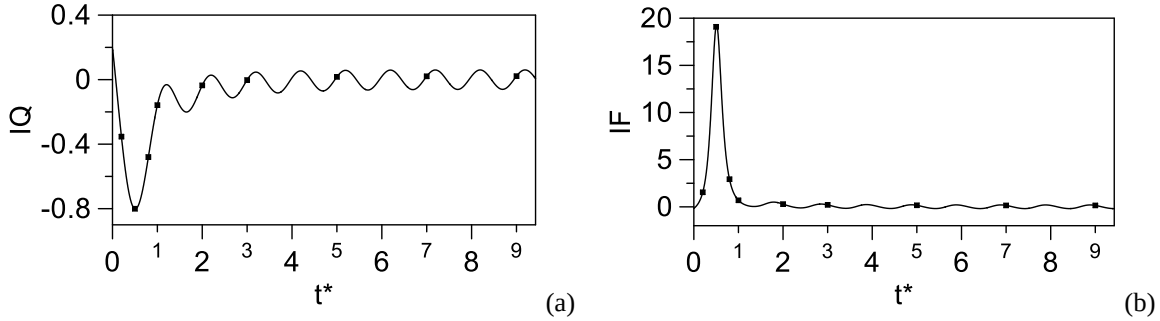

Figure 3.a, b - Comparison between the results obtained by Mathematica (dots) and FORTRAN (lines) for the maximum case
($Y_0 = 1$, $\tau_{R0} = 1$, $\tau_{R1} = 1$).

Knowing the analytic solution (10.c) of the limit case, where the friction factor tends to 16, Fig. 4 shows that the reference case reaches steady state oscillating around said value, which indicates a good response from the mathematical model.

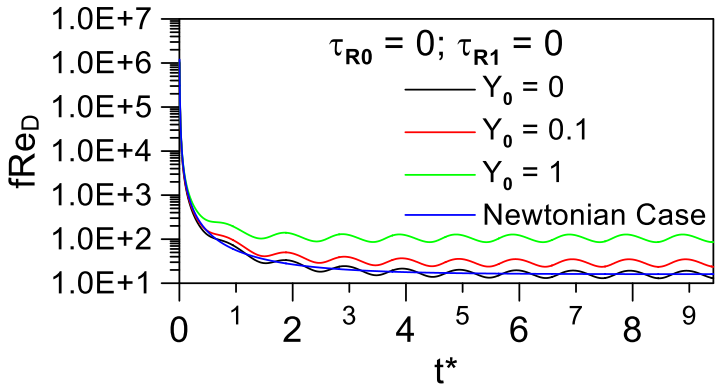

Figure 4. Friction factor versus time for $Y_0 = 0$, 0.1 and 1, $\tau_{R0} = 0$, $\tau_{R1} = 0$, e = 0.2 and for the limit case when e = 0.

To evaluate the influence of the parameters Y_0, τ_{R0}, τ_{R1} on the flow, Figs. 5 - 8 are presented where they show U_{av} and fRe_D in function of the time.

5.1 Analysis of parameter Y_0

In general, it can be observed from Figs. 5 to 8 for U_{av} and fRe_D, that when the dimensionless yield stress Y_0 increases ($Y_0 = 0$ to 1), U_{av} decreases and fRe_D increases. This happens because the radius of the plug flow region increases with the value of Y_0, offering greater resistance to the flow.

5.2 Analysis of parameter τ_{R0}

The influence of the dimensionless relaxation time (τ_{R0}) on the flow does not significantly affect the average velocity in steady state. However, in transient state, the increase of τ_{R0} causes a delay in the development of the average velocity and consequently higher fRe_D. The relaxation time represents the time required for the molecules of the fluid to find a new equilibrium configuration after the start of the flow. Therefore, for small intervals of time there is a certain inertia to be overcome as τ_{R0} increases.

5.3 Analysis of parameter τ_{R1}

Now, we can observe the influence of the dimensionless retardation time (τ_{R1}) in fluid flow. It is noted that the presence of the term τ_{R1} causes a small change in the time required for the flow to reach stability. The delay time represents exactly that.

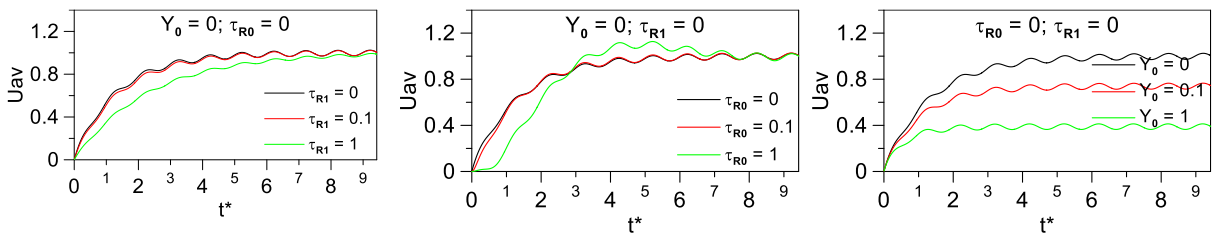

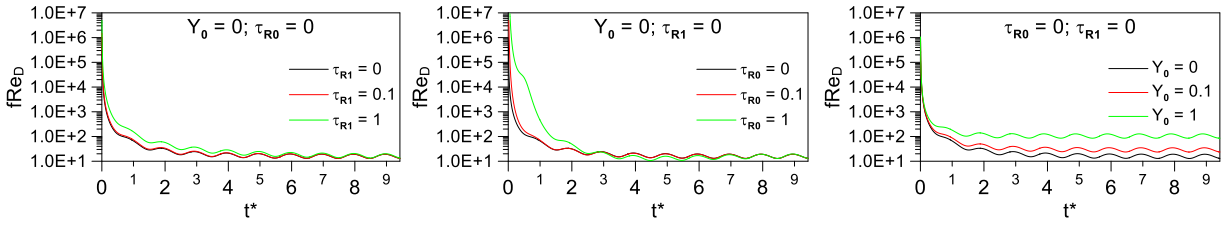

Figure 5. Analysis of the effect of the parameters Y_0, τ_{R0}, τ_{R1} in U_{av} and fRe_D (reference $Y_0 = 0$, $\tau_{R0} = 0$ and $\tau_{R1} = 0$).

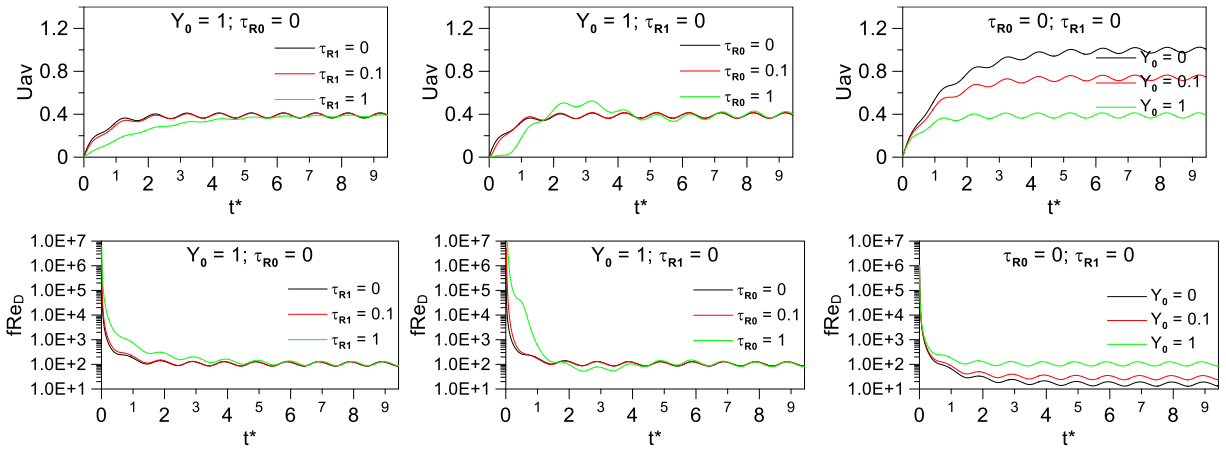

Figure 6. Analysis of the effect of the parameters Y_0, τ_{R0}, τ_{R1} in U_{av} and fRe_D (reference $Y_0 = 1$, $\tau_{R0} = 0$ and $\tau_{R1} = 0$).

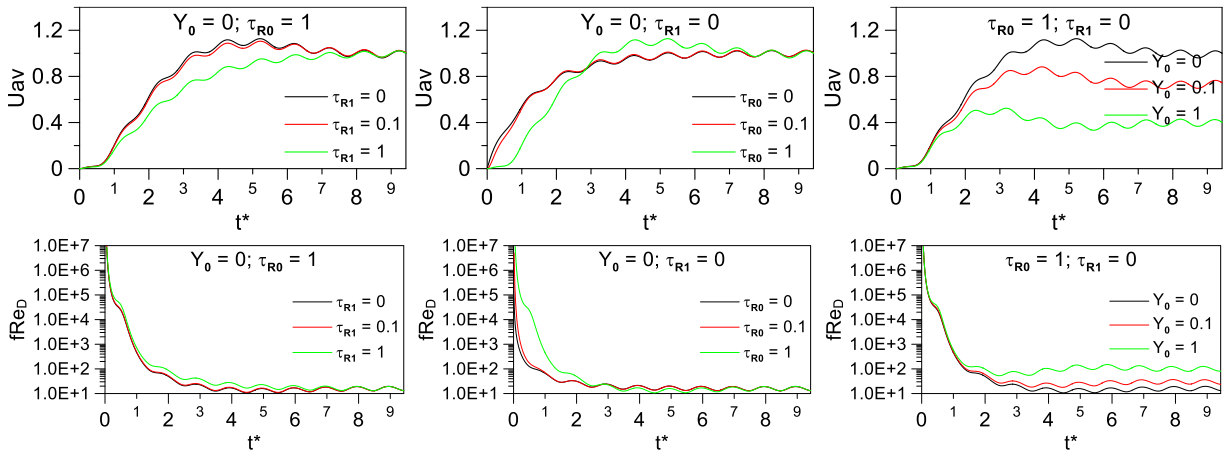

Figure 7. Analysis of the effect of the parameters Y_0, τ_{R0}, τ_{R1} in U_{av} and fRe_D (reference $Y_0 = 0$, $\tau_{R0} = 1$ and $\tau_{R1} = 0$).

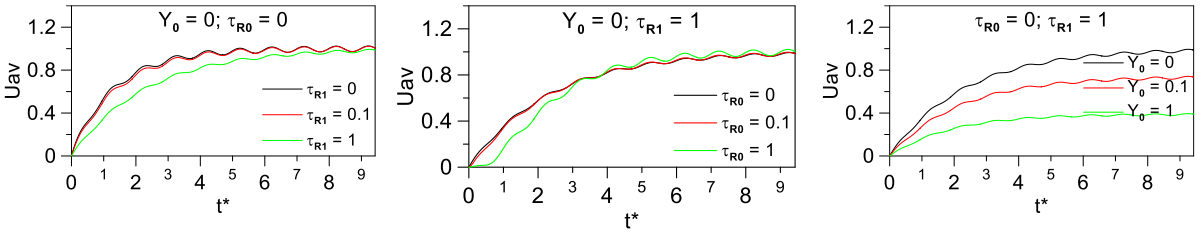

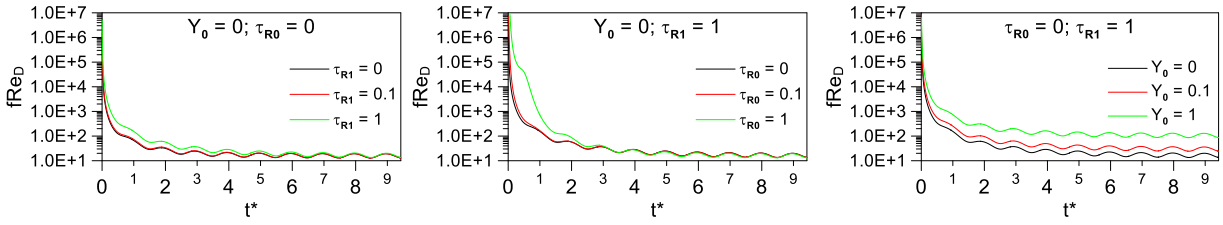

Figure 8. Analysis of the effect of the parameters Y_0, τ_{R0}, τ_{R1} in U_{av} and fRe_D (reference $Y_0 = 0$, $\tau_{R0} = 0$ and $\tau_{R1} = 1$).

6. CONCLUSION

In the present work, we proposed a mathematical model for the blood flow in an artery, with pressure gradient varying periodically in time. In this formulation, the Jeffreys viscoelastic model was used to evaluate the effect of the periodic pressure gradient, along with the Regularized - Casson model for fluid viscosity. To solve the partial differential equation, we used Mathematica's NDSolve and the Method of Lines in FORTRAN language. The results are graphically presented for velocity field, U_{av}, fRe_D, IQ and IF in function of Y_0 (dimensionless yield stress), τ_{R0} (dimensionless relaxation time) and τ_{R1} (dimensionless retardation time). Then, the computer simulations showed that the relationships between the physical quantities described by the model were satisfactory when compared to a limit case previously known. An analysis of influence of the Y_0, τ_{R0} and τ_{R1} in fluid flow showed that the parameter Y_0 and τ_{R0} presented higher importance. The increase of Y_0 reduced the U_{av} and increased the fRe_D, because the radius of the plug flow region increases with the value of Y_0, offering greater resistance to the flow. The τ_{R0} does not significantly affect the average velocity in steady state. However, in transient state, its increase causes a delay in the development of the average velocity and consequently higher fRe_D.

7. REFERENCES

Bird, R.B., Stewart, W.E. and Lightfoot, E. N, 2007. *Transport phenomena*. John Wiley & Sons, Winsconsin, 2nd edition.

Chaturani, P. and Palanisamy, V, 1990. "Pulsatile flow of power-law fluid model for blood flow under periodic body acceleration". *Biorheology*, Vol. 27, p. 747-758.

Fung, Y.C., 1993. *Biomechanics: Mechanical Properties of Living Tissues*. Springer-Verlag, New York, 2nd edition.

Hernandez-Martinez, E., Vernon-Carter, J. and Alvarez Ramirez, J., 2012. "First-harmonic balance for fast evaluation of power-law fluid flow enhancement under periodic pressure gradient". *Chemical Engineering Science*, Vol. 87, p. 67-74.

Humphrey, J.D. and Delange, S.L., 2004. *An Introduction to Biomechanics*. Springer Science and Business Media, New York.

IMSL® FORTRAN Numerical Library, 2014. Version 7.1.0, Rogue Wave Software Inc.,Boulder, USA.

Mitsoulis, E., 2007. "Flows of viscoplastic materials: models and computations". *Rheology Reviews*, p. 135-178.

Maliska, C.R., 2004. *Transferência de Calor e Mecânica dos Fluidos Computacional.* LTC, Brazil.

Misra, J.C. and Pal, B., 1999. "A mathematical model for the study of the pulsatile flow of blood under an externally imposed body acceleration". *Mathematical and Computer Modelling*, Vol. 29, p. 89-106.

Massoudi, M. and Phuoc, T.X., 2008. "Pulsatile flow of blood using a modified second-grade fluid model". *Computers and Mathematics with Applications*, Vol. 56, p. 199–211.

Papanastasiou, T.C., 1987. "Flows of materials with yield". *Journal of Rheology*, Vol. 31, p. 385.

Wolfram Mathematica, 2017. "NDSolve". 6 Mar. 2017 <http://reference.wolfram.com/language/ref/NDSolve.html>.

Zamir, M., 2000. *The Physics of Pulsatile Flow*. Springer-Verlag, New York.

8. RESPONSIBILITY NOTICE

The authors are the only responsible for the printed material included in this paper.